

Fall 2015

# Cordilleran front range structural features in northwest Montana interpreted from vintage seismic 2 reflection data

Mason Porter

*Montana Tech of the University of Montana*

Follow this and additional works at: [http://digitalcommons.mtech.edu/grad\\_rsch](http://digitalcommons.mtech.edu/grad_rsch)



Part of the [Geophysics and Seismology Commons](#)

---

## Recommended Citation

Porter, Mason, "Cordilleran front range structural features in northwest Montana interpreted from vintage seismic 2 reflection data" (2015). *Graduate Theses & Non-Theses*. Paper 51.

This Publishable Paper is brought to you for free and open access by the Student Scholarship at Digital Commons @ Montana Tech. It has been accepted for inclusion in Graduate Theses & Non-Theses by an authorized administrator of Digital Commons @ Montana Tech. For more information, please contact [ccote@mtech.edu](mailto:ccote@mtech.edu).

***Title***

Cordilleran front range structural features in northwest Montana interpreted from vintage seismic reflection data.

***Author names and affiliations***

Mason C. Porter<sup>1</sup>, Bradley S. Rutherford<sup>1</sup>, Marvin A. Speece<sup>1\*</sup>, Jesse G. Mosolf<sup>2</sup>

<sup>1</sup>Montana Tech, Department of Geophysical Engineering, Butte, MT, 59701, United States

<sup>2</sup>Montana Bureau of Mines and Geology, Butte, MT, 59701, United States

***\*Corresponding author***

1300 W. Park St., Butte, MT, 59701

1-406-496-4188

MSpeece@mtech.edu

***Keywords***

Montana, Cordillera, autochthonous, Rocky Mountain trench, seismic reflections

## **Abstract**

Industry seismic reflection data were collected in 1983 in the Rocky Mountain Cordillera front ranges of northwest Montana. These seismic profiles represent 160 km of deep reflection data that cross the eastern Purcell anticlinorium, Rocky Mountain Trench (RMT), Rocky Mountain Basal Detachment (RMBD), and Lewis thrust. We have reprocessed these data using modern processing techniques including refraction statics, pre-stack time migration (PSTM), and pre- and post-stack depth migration. The RMT contains Tertiary fill to 1 km depth and the RMT fault system has a minimum of 3-4 km of normal displacement. The RMT and Flathead fault systems are interpreted to be structurally linked and may represent a synthetic, en echelon extensional fault system. The RMBD is present in every profile with a depth of 8 km in the east and 13 km in the west, dipping 3-10° west. Evidence for the autochthonous Mesoproterozoic Belt supracrustal and basal Cambrian rocks is present in all of the five profiles beneath the RMBD and extends east of the RMT. The Lewis thrust is identified and the sole position of the thrust into the RMBD is interpreted to be east of the RMT.

## 1. Introduction

The Rocky Mountain Cordillera in Northwestern Montana strikes northwest and is characterized by east verging thrust faults and west dipping normal faults. Compressional faults transported a thick slab of Belt-Purcell metasedimentary rocks east out of a Precambrian depositional basin and over Phanerozoic rocks during the late Cretaceous to early Paleocene phase of supracrustal shortening (ex. Yoos et al., 1991; van der Velden and Cook, 1994, 1996; Cook and van der Velden, 1995; Sears 2000; Price and Sears, 2001). The Lewis thrust is an example of a compressional thrust fault extending from northwestern Montana into Alberta, Canada (van der Velden and Cook, 1994). Seismic reflection profiles both to the north and within our study area have been used to interpret the position of the sole point of the Lewis thrust into the Rocky Mountain Basal Detachment (RMBD). The Lewis thrust exits a décollement zone east of the Purcell anticlinorium, a regional structural high that dominates northwest Montana and southwestern Canada.

Previous seismic reflection surveys were used to characterize the major geologic features in the region, including the RMBD (Bally et al., 1966; Yoos et al., 1991, van der Velden and Cook, 1994; Cook and van der Velden, 1995; van der Velden and Cook, 1996). A remarkably massive metasedimentary prism of Belt rocks range from 15 km to more than 20 km thick in the Purcell anticlinorium, and thin eastward to approximately 2 km (Mudge, 1970; Harrison, 1972; McMechan, 1981; Winston and Link, 1993). Harrison et al. (1985) and Yoos et al. (1991) showed no significant thickness of Paleozoic rocks beneath the eastern Purcell anticlinorium, west of the Rocky Mountain Trench (RMT). The RMT is a 1600 km topographic low bounded on the east by west dipping listric normal faults formed during a phase of supracrustal extension that initiated 1-5 m.y. after contractional deformation ceased (Constenius, 1996). The RMT

coincides with the autochthonous eastern margin of the Belt basin where a wedge of undeformed, shelfal Beltian sediments was interpreted to exist beneath the RMBD and above North American crystalline basement; however, estimates of the lateral extent of the autochthonous wedge have varied (Bally et al., 1966; Yoos et al., 1991; van der Velden and Cook, 1994, 1996, Constenius, 1996).

160 km of two-dimensional deep seismic reflection profiles were acquired by Techco Incorporated in 1983 (Figure 1). Using modern techniques, we reprocessed five Techco profiles that cross the eastern Purcell anticlinorium, the RMT, and the Lewis thrust sheet in northwest Montana. In this paper, we present an analysis of the reprocessed seismic reflection data and interpretation of major structural features observed in these profiles. This information provides insights into (1) the structural geology of the RMT; (2) the depth of the RMBD; (3) the position where the Lewis thrust departs the décollement zone; and (4) the autochthonous eastern margin of the Belt basin.

## **2. Geologic Background**

Rocks in the study area consist mainly of the metasedimentary Belt Supergroup strata (Figure 1,2,3). The Belt Supergroup sediments, correlative of the Purcell Group in Alberta and British Columbia, are Mesoproterozoic metasedimentary rocks that crop out in Idaho, Washington, and Montana. The thickness of the Belt Supergroup sedimentary rocks have been estimated to be 15-22 km to the west of our study area (Yoos et al., 1991). The Supergroup sequence has been divided into four subgroups, from oldest to youngest: lower Belt, Ravalli Group, middle Belt, and Missoula Group (Figure 3).

Metamorphism has altered the Belt Supergroup from claystones, shales, siltstones and sandstones into dense argillites, siltites, and quartzites (Harrison, 1972). The mostly

metamorphosed lower Belt, Ravalli Group and Missoula Group are composed of mostly quartzites, siltites and argillites, while the middle Belt is composed of mostly dolomitic carbonates (Harrison, 1972; Cressman, 1989). High gravity anomalies and strong reflection events observed in the anticlinorium were first interpreted as buried thrust sheets of dense Paleozoic carbonates; seismic surveys near the study area and well data from the Arco-Marathon Paul Gibbs #1 well (Figure 4) instead identified metaclastic sediments of the lower Belt frequently intruded by gabbroic to dioritic sills, which caused both the higher gravity readings and strong reflection events (Harris, 1985; Boberg et al., 1989; Cressman, 1989; Yoos et al., 1991). The injected mafic sills have been estimated to be approximately 1400 Ma (Anderson and Davis, 1995; Brown and Woodfill, 1998; Luepke and Lyons, 2001). The sills are easily identified in geophysical logs as zones of relatively low radioactivity, high compressional velocity (~6800 m/s), and high density (~3.0 g/cm<sup>3</sup>) within a fairly consistent Belt background (~5200 m/s and ~2.7 g/cm<sup>3</sup>) which create strong reflection events as seen in the synthetic seismogram.

The Purcell anticlinorium is a regional scale anticline formed in the hanging wall of the RMBD during Mesozoic and Early Tertiary crustal shortening (van der Velden and Cook, 1996). In Canada, the anticlinorium was described by Price (1981) as the inverted Belt basin displaced onto the continental platform and draped across the Precambrian rift controlled basin margin. Sears and Buckley (1993), Sears (2000, 2001, 2004, 2007) and Price and Sears (2001) adopted an equivalent model in Montana suggesting that the axis of a basement megaramp coincides with the axial trace of the anticlinorium. Alternatively, Constenius (1996) and Fuentes et al. (2012) interpreted the Purcell anticlinorium as a fault-bend fold above a significant wedge of autochthonous Belt rocks. Time-structural contours based on seismic data of the crystalline basement from Cook and van der Velden (1995) and the RMBD from van der Velden and Cook

(1996) indicate the basement megaramp begins to ramp down east of the axial trace of the Purcell anticlinorium. Ainsworth (2009) used gravity and seismic data over the northern limb of the Purcell anticlinorium, specifically the Moyie anticline in southeastern British Columbia, to conclude that thickened lower Belt rocks above deep basement comprised the core of the anticlinorium.

The RMT is a 1600 kilometer linear topographic low in southwestern Canada and northwestern Montana that has been defined as the structure that separates the Purcell anticlinorium from the western front ranges (Cook and van der Velden, 1995; van der Velden and Cook, 1996). The RMT is an extensional half graben, bounded to the east by the RMT normal fault system. The southern RMT fault system is composed of a series of extensional faults with normal displacements of 7-12 kilometers near 49°N latitude (van der Velden and Cook, 1996). The style of faulting in the southern RMT is markedly different than the strike-slip motion faults comprising the northern RMT in Canada. The extensional faults that formed the southern RMT cut the eastern Purcell anticlinorium during middle to late Tertiary. The most recent movement on the RMT fault system deformed Miocene strata. Previous interpretations of the RMT suggest the topographic low is a zone of crustal weakness formed along an ancient continental margin (van der Velden and Cook, 1996). Extension has been accommodated primarily by listric normal faults on the east side of the trench that are commonly compensated by antithetic faults to the west. The extensional faults formed prominent west-facing mountain scarps and have merged with and reactivated the compressional detachment near the hinge line of the RMBD ramp (Constenius, 1996; van der Velden and Cook, 1996; Lageson and Stickney, 2000).

Beginning approximately 70-75 Ma, the Lewis thrust fault transported 7-8 km of Belt Supergroup rocks east over a footwall of complexly imbricated Paleozoic and Mesozoic strata during a 15 m.y. period of local crustal shortening (Constenius, 1996; Sears, 2001). The 457 km Lewis thrust was first mapped by Willis (1901) from exposures in Glacier National Park, where it strikes N40°E. The Lewis thrust is a low-angle folded thrust fault where, in the area of greatest displacement, the minimum slip is 65 km (van der Velden and Cook, 1994). Yoos et al. (1991) used an unmigrated vibroseis reflection profile (WTF-82-1, Figure 1) that crossed the western front ranges to interpret the subsurface position of the Lewis thrust.

One hypothesis suggests that the entire Belt Supergroup was not transported eastward, but rather an autochthonous wedge of shelfal Belt rocks was left in place (van der Velden and Cook, 1994, 1996; Fuentes et al., 2012). Reflections beneath the Lewis sheet and the RMBD but above North American crystalline basement were interpreted as both autochthonous Cambrian and Belt rocks (Bally et al, 1966; van der Velden and Cook, 1994, 1996). Where the reflective package beneath the RMBD appeared thicker than a few hundred meters, autochthonous Belt rocks must be included beneath the basal Cambrian event in the reflective zone (Yoos et al., 1991). Interpreted seismic data collected in southern Canada (Profile 2, Figure 1) shows a wedge of autochthonous Belt rocks (van der Velden and Cook, 1994, 1996).

The Flathead fault was interpreted by Bally et al. (1966) to be an extensional reactivation of a major ramp in the Lewis thrust in the hinterland of the Lewis thrust salient. The Flathead duplex structure created a footwall ramp in the Lewis thrust that was subsequently reactivated by the Flathead normal fault during Tertiary crustal extension (Bally et al., 1966; Gordy et al., 1977). Slip on the Flathead extensional fault system exceeded 15 km, displacing the Lewis thrust sheet and creating the deep (> 3 km of Tertiary fill) Kishenehn extensional basin (Constenius,



1982, 1988). The eastern margin of the Kishenehn basin is bounded by the Nyack fault that was formed antithetic to the Flathead fault system.

### **3. Seismic Data**

#### *3.1 Acquisition*

Five seismic profiles acquired by Techco, Inc. in 1983 delineate features of the Purcell anticlinorium, the RMT, the Hefty thrust, and the Lewis thrust. The data were collected in Northwest Montana, north of Flathead Lake (Figure 1,2). These data represent 160 linear kilometers collected by Rocky Mountain Geophysical and Signal of Montana on behalf of Techco Incorporated, formerly Transcon Energy. The data were collected in the area because of the excellent production of the Waterton gas field in southern Alberta in the 1950s, which prompted more exploration to identify the western extent of buried thrust sheets of Phanerozoic rocks (Fritts and Klipping, 1987; van der Velden and Cook, 1994).

The four southernmost profiles (83-101, 83-103, 83-104, 83-105) were acquired using the Poulter method. Typically a 30 lb. load of dynamite one meter above the ground surface provided the source energy for the lines. All these profiles strike in the same SW-NE direction and helicopters were used to transport equipment through the mountainous terrain. The northernmost line, 83-201V, used a vibroseis source with a frequency sweep of 56 to 14 Hz and was collected along an established road. The field acquisition parameters of the dataset are shown in Table 1.

#### *3.2 Processing*

These data were originally donated to Montana Tech in the form of 9 track tape and subsequently converted from tape to digital SEG-Y format. We processed the data according to standard CMP processing procedures (Table 2). Migration artifacts created by the pre-stack

migration algorithm in 83-101 and 83-104 dominated the images; therefore, post-stack time migrated sections were stretched to depth using velocity models created for depth migration and were used as our preferred sections for interpretation. The crooked geometry of 83-201V did not allow the use of a pre-stack depth migration algorithm, so the pre-stack time migrated section was stretched to depth using depth migration velocity model. Two lines (83-103, 83-105) used a pre-stack depth migration algorithm (Table 2).

Strong air-wave energy was produced from using above ground dynamite sources for the four seismic profiles that used the Poulter method. A tail mute was applied to remove the airwave because useful reflections were not otherwise recoverable after the airwave. Raw records were often plagued with cable noise and high energy noise bursts. Once the traces were edited and balanced, threshold median noise removal of noise and signal replacement algorithm (THOR) was used to further reduce noise (Butler, 2012).

### *3.3 Interpretation*

#### *3.3.1 Profile 83-201V*

Profile 83-201V (Figure 5) is a 33.8 km long vibroseis seismic line that was surveyed near the US-Canada border. The northernmost profile of this study is curved because the vibroseis source required a road. Although the upper half of the profile is reflective, most of the reflections are most likely contained within Belt Supergroup rocks and identify changes in lithology. This analysis is in agreement with Yoos et al. (1991) for their interpretation of a nearby profile (WTF-82-1). A minor reactivated normal fault occurs 5 km from the western side of the profile; the slip on this fault is 500 m. A major thrust fault interpreted as the Hefty thrust translated Belt rock over Paleozoic rocks with a slip of approximately 4 km. 83-201V crosses the Hefty thrust then curves along strike of the fault providing a high quality image of the footwall

of the Hefty thrust. The MacDonald thrust branches from the Hefty thrust and extends eastward, with minor thrust faults in the Paleozoic rocks on the eastern side of the section.

The RMBD is clearly seen across the profile at 8.5 km deep on the east side of the profile. The RMBD dips west on the western side of the section at 3°. Reflections interpreted as the Lewis thrust are seen on the eastern side of the profile. Beneath the RMBD, reflections indicating autochthonous rock are present and are interpreted as a thin veneer of basal Cambrian rock and a wedge of autochthonous Belt rock.

### *3.3.2 Profile 83-101*

Profile 83-101 (Figure 6) is the northernmost Poulter method line with a length of 45.6 km. This profile extends from the eastern Purcell anticlinorium through the Whitefish Range to the edge of the Kishenehn Basin (Figure 1). Loss of coherent data near the western edge of the profile is caused by signal attenuation due to the low velocity sediments that have filled the RMT. Faint reflections show the depth of fill to be 0.8-1.0 km. The RMBD can be seen along nearly the entire length of the entire profile, at a depth of 8.5-11 km. An increase in reflectivity beneath the western part of the RMBD where the dip of the detachment has increased is interpreted to be an autochthonous wedge of Belt rock.

The Hefty thrust cuts through most of the profile, with a series of normal faults soling into the thrust fault on the eastern edge of the profile. The Hefty thrust has a slip approximately 5.5 km based on sill offset, and this offset was used to interpret the other Poulter method profiles. We have interpreted reflections on the eastern side of the profile above the décollement to outline the Lewis thrust. The position where the Lewis thrust exits the décollement zone is not clearly seen, but we have made an interpretation consistent with Gordy et al., (1977), Yoos et al.,

(1991), and van der Velden and Cook (1994). A west tapering wedge beneath the Lewis thrust and above the west dipping ( $\sim 3\text{-}4^\circ$ ) RMBD we have interpreted as Paleozoic rocks.

All reflections above the décollement on the western side of the profile are interpreted to represent mafic sills encased in the lower Belt. The sills appear to be cut by the RMT fault and continue after an apparent normal dip-slip of approximately 3 km.

### *3.3.3 Profile 83-103*

Profile 83-103 (Figure 7) is located 21 km southeast of and parallel to 83-101. 83-103 does not cross the RMT or the Kishenehn Basin (Figure 1). Reflections above the décollement dominating the western side of the section are interpreted as mafic sills ranging from 5-8 km in depth from the surface. Reflections present on the eastern edge of the section have been interpreted as the Lewis thrust leaving the décollement. The Hefty thrust can also be seen throughout the whole profile, with a slip of 5.5 km along the fault surface, based on the interpretation of the Hefty thrust in 83-105. The RMBD can be clearly seen throughout the profile at approximately 8-10 km in depth. Beneath the RMBD, strong reflections are interpreted to be the autochthonous rock consisting of basal Cambrian and the underlying autochthonous Belt units.

### *3.3.4 Profile 83-104*

Profile 83-104 (Figure 8) lies parallel to 83-101 and 30 km to the southeast. Faults observed near the middle of the profile have been interpreted as the RMT fault system. The easternmost RMT fault has a normal dip-slip of 2.8 km. Other faults interpreted to be part of the RMT fault system have been mapped west of the RMT (Figure 2), but 83-104 does not extend far enough west for the line to intersect these faults.

In the upper part of the section, a reflection outlining the Tertiary fill-Belt rock contact is clearly seen at 0.7-0.9 km. The Whitefish fault has been interpreted to have a thrust offset of ~1.5 km. The RMBD can be seen throughout the entire profile at 8-11 km in depth. We have interpreted the zone of reflectivity beneath the basal detachment in the west as the autochthonous wedge of Belt rock, with North American basement rock underneath.

#### *3.3.5 Profile 83-105*

Profile 83-105 (Figure 9) is the southernmost profile, located 38.5 km southeast of 83-101. The basal detachment can be seen on the eastern side of the profile at 8 km deep. The RMBD dips westward to 13.5 km deep near the western edge of the profile, with a 5° increase in dip near where the RMT extensional faults sole into the RMBD.

Reflections on the western half of the section have been interpreted as mafic sills. The sills truncate against faults dipping westward, then continue east until the middle of the profile. The normal dip-slip offset of the sills against the faults is 3.5 km. The RMT can also be identified by the loss of coherent reflections beneath the trench. A series of extensional faults occurs throughout the RMT.

The RMT fault system cuts a thrust fault that previously thrust older Belt eastward onto other Belt rock. The fault has been reactivated as a normal fault, and projects onto the Whitefish fault on the surface. We interpret that the Hefty thrust soles into the RMBD east of the RMT and immediately west of the Lewis thrust. The Lewis thrust is delineated by faint reflections above the décollement, but the exact position where the thrust soles into the RMBD is not clearly imaged. We have interpreted reflections beneath the RMBD as the outline of the autochthonous wedge of Belt rock.

#### 4. Discussion

The uppermost portions of the profiles are generally lower quality with low reflectivity; the exception being the vibroseis sourced profile 83-201V. The upper Belt rocks were noted by Yoos et al. (1991) to be unreflective in 2 profiles near the study area, west of the RMT. Yoos et al. (1991) also observed moderately reflective zones interpreted within the middle Belt carbonates and Missoula Group east of the RMT. In our profiles we observe a northward and eastward increase in reflectivity of Belt sedimentary contacts that likely represents a transition from deep basinal to shelfal depositional facies. Rapid facies changes and sharp sedimentary contacts observed in the Lewis thrust salient were interpreted to be a result of deposition on a continental shelf (Harrison et al., 1998). We interpret the increased sedimentary reflectivity in our profiles to be related to the sharp contacts characteristic of a shelfal depositional environment that suggests a northeastward shoaling of the Belt basin. Similarly, we observe autochthonous shelfal Belt rock in the footwall of the RMBD to be strongly reflective in several of our seismic sections, and this is consistent with what is shown in Profile 2 (van der Velden and Cook, 1994, 1996).

The RMT fault system is interpreted in 3 of the 5 profiles: 83-101, 83-104, and 83-105. Poor signal within the southern RMT is likely related to signal attenuation through unconsolidated sediments (Harrison et al., 1985; Yoos et al., 1991; van der Velden and Cook, 1994; Cook and van der Velden 1995). Poor source coupling using the Poulter method is an additional potential cause for the weak signal penetration specific to these data. In Profile 83-104, a reflection event near the surface in the RMT has been identified as the stratigraphic boundary between the dense Belt Supergroup rock and the unconsolidated Tertiary fill. The depth to the Belt-Tertiary sedimentary fill boundary is interpreted to be 0.7-0.9 km. Although the

Belt-fill boundary is clearly evident in 83-104, reflections identified as the Belt-Tertiary boundary within the RMT are also present in 83-101 and show a depth to the top of the Belt rocks of 0.8-1.0 km.

Major reflections on the profiles western edges have been interpreted as mafic intrusive sills. Sills on the western edge of 83-101, generally 5-9 km deep, and sills on the western side of 83-105, generally 4-9 km deep, truncate against the RMT fault, then continue in the foot wall indicating normal dip-slip of 3 km and 3.5 km, respectively. Reflections observed from the sills are not as pronounced east of the RMT because the sills terminate in Belt rocks. The RMT fault system likely soles into the décollement near the approximate position of the hinge of the RMBD suggesting the RMT fault system preferentially reactivated the RMBD. Figure 10 shows a model for the tectonic development of the southern RMT.

Throughout every profile, the RMBD can be seen and is clearly defined east of the RMT. The décollement on the western sides of the sections, specifically beneath the RMT, becomes more difficult to interpret. The depth to the RMBD is 8-10 km deep east of the RMT dipping at  $\sim 3^\circ\text{W}$ , and increases to as much as  $\sim 10^\circ$  west of the trench. We assume the  $10^\circ$  dip west of the trench remains approximately constant until the RMBD reaches the maximum depth of the Belt basin ( $> 20$  km deep) (van der Velden and Cook, 1994). Beneath the RMBD, we interpret a thin veneer of basal Cambrian that causes a strongly reflective event that is seen in every profile. The autochthonous Paleozoic rocks were first mentioned by Bally et al. (1966) and range in thickness from tens to hundreds of meters (Yoos et al, 1991). Evidence for the autochthonous Belt rocks has been shown in all of the five profiles interpreted in this study. A westward thickening reflection package beneath the RMBD includes the basal Cambrian and autochthonous Belt rocks.

The western edge of the Lewis thrust is present in four of the five profiles, the exception being 83-104 because the seismic section does not extend far enough east. Although seismic reflections interpreted to be the Lewis thrust are faint and the exact location where the Lewis thrust soles into the RMBD is not clearly outlined, our interpretation agrees with previous interpretations of other seismic data near our study area (Gordy et al., 1977; Yoos et al., 1991; van der Velden and Cook, 1994, 1996). We interpret the western extent of the allochthonous Paleozoic rocks at the sole point of the Lewis thrust into the RMBD, which occurs east of the RMT. The Lewis thrust dips 8-10° W in the four profiles.

Palinspastic restorations completed by van der Velden and Cook (1994, 1996) restore the Lewis thrust west of the trench with the autochthonous Belt and Paleozoic wedge present, and their position of the autochthonous Belt rocks approximately agrees with our interpretation. We have interpreted the autochthonous basin margin décollement ramp (dip change beneath the RMT) to be beneath or slightly to the west of the RMT, significantly (40-50 km) farther east than the interpretation of Constenius (1996), Sears (2000, 2001, 2004, 2007) and restorations completed by Price and Sears (2001). Our interpretation of the geometry of the wedge is largely based on the interpretation of van der Velden and Cook (1994, 1996) and includes only a minor wedge of shelfal Belt rocks in contrast to the extensive wedge proposed by Constenius (1996), which is thicker and ramps down slightly west of the Arco Marathon Paul Gibbs #1 well.

The Whitefish fault is seen on the two southernmost profiles, 83-104 and 83-105. To the east of 83-103 on the geologic map, lower Belt has been thrust over middle Belt, with minimum eastward displacement of approximately 3.5 km. We have interpreted the Whitefish fault to have been later reactivated as a normal fault (Figures 8 and 9); however, the Whitefish fault still



preserves ~1.5 km of thrust displacement (profile 83-104). The Whitefish thrust in profile 83-105 has been reactivated as a normal fault with a minimum slip of ~500 m.

Figure 11 is a simplified schematic that shows the orientation of the RMT and the Flathead fault systems and their associated slip vectors. This figure was created by compiling our results with results to the north and east of our study area that were reported in previous studies (Constenius, 1982; van der Velden and Cook, 1996). The RMT and Flathead fault system are related and as the Flathead fault slip increases, the RMT fault slip decreases. These faults are interpreted to be structurally linked and may represent a synthetic, en echelon extensional fault system.

## **5. Conclusions**

Evidence for the RMT fault system is present in three of the five profiles. Injected mafic sills of greater than 1000 Ma have been normally offset approximately 3-4 km by the RMT extensional fault system. Reflections in the upper sections of two profiles outline the boundary between the Belt and Tertiary fill, with a maximum thickness of 0.7-1 km. The RMT fault and Flathead fault systems are most likely structurally linked and could represent a synthetic en echelon extensional fault system.

The RMBD can be seen in each profile, with depth averaging 8 km and a ~3-4° W dip east of the RMT, and a depth of approximately 13 km with a dip of ~10°W west of the trench. A start of a major décollement ramp occurs beneath or slightly west of the RMT. RMT faults sole into the RMBD at or slightly west of the hinge point, suggesting the RMT fault system preferentially reactivated the RMBD near the ramp. The Lewis thrust can be seen in four of the five profiles. The dip of the thrust is consistent at 8-10° W. Although the exact locations of where the Lewis thrust soles into the RMBD are unclear, our interpretations are consistent with

other interpreted seismic profiles of higher quality (van der Velden and Cook, 1994). The Lewis thrust soles into the RMBD to the east of the Rocky Mountain Trench where the thrust separates allochthonous Paleozoics and overthrust Belt rocks on four of the profiles.

Reflections beneath the RMBD support the existence of an autochthonous Belt wedged between the décollement and North American basement. Evidence of the autochthonous wedge is present in all of the profiles, but the profiles do not extend far enough west and therefore do not fully outline the autochthonous Belt. Our interpretation of the location and depth of the autochthonous Belt is in agreement with the interpretations of van der Velden and Cook (1994, 1996).

## **6. Acknowledgements**

These data were donated to Montana Tech by Hugo Pulju, with assistance by Ed Pulju. Skye Callantine arranged for a generous donation from Chesapeake Energy to transcribe field records for these data from nine-track tape. We thank Eric Johnson for preparing a detailed tax appraisal of these data. These data were processed using VISTA™ seismic data processing software donated to Montana Tech by Schlumberger.

## References

Ainsworth, H.L., 2009. Structure of the Moyie Anticline delineated on a grid of reflection seismic profiles in southeastern British Columbia. Master's thesis, University of Calgary.

Anderson, H. E., Davis, D. W., 1995. U-Pb geochronology of the Moyie sills, Purcell Supergroup, southeastern British Columbia: implications for the Mesoproterozoic geological history of the Purcell (Belt) basin. *Canadian Journal of Earth Sciences* 32 (8), 1180-1193.

Bally, A.W., Gordy, P.L., Stewart, G.A., 1966. Structure, seismic data, and orogenic evolution of southern Canadian Rocky Mountains. *Bulletin of Canadian Petroleum Geology* 14 (3), 337-381.

Boberg, W.W., Frodesen, E.W., Lindecke, J.W., Hendrick, S.J., Rawson, R.R., Spearing, D.R., 1989. Stratigraphy and tectonics of the Belt basin of western Montana: Evidence from the Arco-Marathon No. 1 Paul Gibbs well, Flathead County, Montana. *Montana Geological Society 1989 Field Conference, Montana Centennial Edition* 1, 217-229.

Brown, D.A., Woodfill, R.D., 1998. The Moyie industrial partnership project; geology and mineralization of the Yaak–Moyie Lake area, southwestern British Columbia. *Geological Survey Canada Geologic Fieldwork* 9, 22.

Butler, P., 2012. Strong noise- removal and replacement on seismic data. *Canadian Society of Petroleum Geologists, Geo-Convention 2012: Vision*.

391 Constenius, K.N., 1982. Relationship between the Kishenehn basin, and the Flathead listric normal fault  
 392 system and the Lewis thrust salient: Geologic studies of the Cordilleran Thrust Belt. Rocky Mountain  
 393 Association of Geologists, 817– 830.  
 394

395 Constenius, K.N., 1988. Structural configuration of the Kishenehn Basin delineated by geophysical  
 396 methods, northwestern Montana and southeastern British Columbia. Mountain Geologist 25, 13–28.  
 397

398 Constenius, K.N., 1996. Late Paleogene extensional collapse of the Cordilleran foreland fold and thrust  
 399 belt. Geological Society of America Bulletin 108, 20-39.  
 400

401 Cook, F.A., van der Velden, A.J., 1995. Three-dimensional crustal structure of the Purcell Anticlinorium in  
 402 the Cordillera of southwestern Canada. Geological Society of America Bulletin 107, 642-664.  
 403

404 Cressman, E.R., 1989. Reconnaissance stratigraphy of the Prichard Formation (Middle Proterozoic) and  
 405 the early development of the Belt Basin, Washington, Idaho, and Montana. United States Geological  
 406 Survey Professional Paper, 1490.  
 407

408 Fritts, S.G., Klipping, R.S., 1987. Structural interpretation of northeastern Belt basin: implications for  
 409 hydrocarbon prospects. Oil & Gas Journal 85 (39), 75–79.  
 410

411 Fuentes, F., DeCelles, P.G., Constenius, K.N., 2012. Regional Structure and kinematic history of the  
 412 Cordilleran fold thrust belt in northwestern Montana, USA. Geosphere 8 (5), 1104-1128.  
 413

414 Gordy, P.L., Frey, F.R., Norris, D.K., 1977. Geologic guide for the Canadian Society of Petroleum  
 415 Geologists 1977 Waterton-Glacier Park field conference. Canadian Society of Petroleum Geologists.  
 416  
 417 Harris, D.W., 1985. Crustal structure of northwestern Montana. Master's thesis, University of Montana.  
 418  
 419 Harrison, J.E., 1972. Precambrian Belt basin of northwestern United States; Its geometry, sedimentation  
 420 and copper occurrences. Geological Society of America Bulletin 83, 1215-1240.  
 421  
 422 Harrison, J.E., Cressman, E.R., Kleinkopf, M.D., 1985. Regional structure, the Atlantic Richfield-Marathon  
 423 Oil No. 1 bore-hole, and hydrocarbon resource potential west of the RMT in northwestern Montana.  
 424 USGS Open-File Report 85-249.  
 425  
 426 Harrison, J.E., Griggs, A.B., and Wells, J.D., 1986. Geologic and structure maps of the Wallace 1° × 2°  
 427 quadrangle, Montana and Idaho. U.S. Geological Survey Miscellaneous Investigations Map I-1509, scale  
 428 1:250,000.  
 429  
 430 Harrison, J.E., Cressman, E.R., Whipple, J.W., 1992. Geologic and structure maps of the Kalispell 1° x 2°  
 431 quadrangle, Montana, and Alberta and British Columbia. United States Geological Survey Geologic  
 432 Quadrangle Map I-2267, scale 1:250,000.  
 433  
 434 Harrison, J.E., Whipple, J.W., Lidke, D.J., 1998. Geologic map of the western part of the Cut Bank 1° × 2°  
 435 quadrangle, northwestern Montana. U.S. Geological Survey Geologic Investigations Series I-2593, scale  
 436 1:250,000.  
 437

438 Lageson, D.R., Stickney, M.C., 2000. Seismotectonics of Northwest Montana, USA. Montana Geological  
 439 Society 50<sup>th</sup> Anniversary Symposium: Montana/Alberta Thrust Belt and Adjacent Foreland, 109-126.  
 440  
 441 Luepke, J.J., Lyons, T.W., 2001. Pre-Rodinian (Mesoproterozoic) supercontinental rifting along the  
 442 western margin of Laurentia: geochemical evidence from the Belt-Purcell Supergroup. Precambrian  
 443 Research, 111, 79-90.  
 444  
 445 Massey, N.W.D., MacIntyre, D.G., Desjardins, P.J., Cooney, R.T., 2005. Digital Geology Map of British  
 446 Columbia: Whole Province: B. C. Ministry of Energy and Mines, Geofile 2005-1. (SCALE)  
 447  
 448 McMechan, M.E., 1981. The Middle Proterozoic Purcell Supergroup in the southwestern Rocky and  
 449 southeastern Purcell Mountains, British Columbia and the initiation of the Cordilleran miogeocline,  
 450 southern Canada and adjacent United States. Bulletin of Canadian Petroleum Geology, 29 (4), 583-621.  
 451  
 452 Mudge, M.R., 1970. Origin of the Disturbed Belt in northwestern Montana. Geological Society of  
 453 America Bulletin, 81, 377-392.  
 454  
 455 Mudge, M.R., Earhart, R.L., Whipple, J.W., Harrison, J.E., 1982. Geologic and structure map of the  
 456 Choteau 1° × 2° quadrangle, western Montana. U.S. Geological Survey Miscellaneous Investigation Series  
 457 Map I-1300, scale 1:250,000.  
 458  
 459 Price, R.A., 1981. The Cordilleran foreland thrust and fold belt in the southern Canadian Rocky  
 460 Mountains. In MacClay, K. R., Price, N.J. (Eds.), Thrust and nappe tectonics: Geological Society of London  
 461 Special Publication, 9, 427-448.

462

463 Price, R.A., Sears, J.W., 2001. A preliminary palinspastic map of the Mesoproterozoic Belt-Purcell

464 Supergroup, Canada and USA: Implications for the tectonic setting and structural evolution of the Purcell

465 Anticlinorium and the Sullivan deposit. In Lydon, J. W., Hoy, T., Slack, J. F., and Knapp, M.E. (Eds.), The

466 Sullivan deposit and its geological environment: St. John's, Canada, Geological Association of Canada,

467 Mineral Deposits Division, Special Publication 1, 61-81.

468

469 Sears, J.W., Buckley, S.N., 1993. Cross-section of the Rocky Mountain thrust belt from Choteau to Plains,

470 Montana: Implications for the geometry of the eastern margin of the Belt basin. Belt Symposium III:

471 Spokane Washington Belt Association.

472

473 Sears, J.W., 2000. Rotational kinematics of the Rocky Mountain thrust belt of Northern Montana.

474 Montana Geologic Society 50<sup>th</sup> Anniversary Symposium, 1, 143-149.

475

476 Sears, J.W., 2001. Emplacement and denudation history of the Lewis-Eldorado-Hoadley thrust slab in the

477 northern Montana Cordillera, USA: Implications of steady-state orogenic processes. American Journal of

478 Science, 301, 35-373.

479

480 Sears, J.W., Price, R.A., Khudoley, A.K., 2004. Linking the Mesoproterozoic Belt-Purcell and Udzha basins

481 across the west Laurentia–Siberia connection. Precambrian Research, 129 (3), 291-308.

482

483 Sears, J.W., 2007. Belt-Purcell basin: Keystone of the Rocky Mountain fold-and-thrust belt, United States

484 and Canada. Geological Society of America Special Papers, 433, 147-166.

485

486 van der Velden, A.J., Cook, F.A., 1994. Displacement of the Lewis thrust sheet in southwestern Canada:  
 487 New evidence from seismic reflection data. *Geology*, 22, 819-822.  
 488  
 489 van der Velden, A.J., Cook, F.A., 1996. Structure and tectonic development of the southern Rocky  
 490 Mountain Trench. *Tectonics* 15, 517-544.  
 491  
 492 Vuke, S.M., Porter, K.W., Lonn, J.D., Lopez, D.A., 2007. Geologic Map of Montana. Montana Bureau of  
 493 Mines and Geology Geologic Map 62B, scale 1:500,000.  
 494  
 495 Willis, B., 1901. Oil of the northern Rocky Mountains. *Engineering and Mining Journal*, December 14,  
 496 782-784.  
 497  
 498 Winston, D., Link, P.K., 1993. Middle Proterozoic rocks of Montana, Idaho and eastern Washington: The  
 499 Belt Supergroup. In: Reed Jr., J.C., Bickford, M.E., Houston, R.S., Link, P.K., Rankin, D.W., Sims, P.K., Van  
 500 Schmus, W.R. (Eds.), *Precambrian: Conterminous U.S.* Geological Society of America, Boulder, Colorado,  
 501 487-517.  
 502  
 503 Yoos, T.R., Potter, C.J., Thigpen, J.L., Brown, L.D., 1991. The Cordilleran foreland thrust belt in  
 504 northwestern Montana and northern Idaho from COCORP and industry seismic reflection data.  
 505 *American Association of Petroleum Geologists Bulletin* 75, 1089-1106.



## Figure Captions

**Figure 1.** A simplified geologic map of northwestern Montana and nearby areas. The location of the reprocessed seismic lines and other seismic lines are shown. The Arco-Marathon well that proved the existence of sills is shown, as well as major geologic features and faults such as the Purcell Anticlinorium, Rocky Mountain Trench, Kishenehn Basin, and the Lewis Salient. RMTF – RMT fault, HT – Hefty thrust, FF – Flathead fault (Harrison et al., 1986; Harrison et al., 1992; Harrison et al., 1998; Mudge et al., 1982; van der Velden and Cook, 1994; Massey et al., 2005; Vuke et al., 2007).

**Figure 2.** Detailed geologic map of the study area where the seismic data were collected. This map provided the surface data used in the interpretation of the profiles (modified from Harrison et al., 1992).

**Figure 3.** Regional stratigraphic column and geochronometric ages of Belt-Purcell Supergroup strata. The lower Belt is frequently intruded by sills approximately 1400 Ma (modified from Luepke and Lyons, 2001) (Anderson and Davis, 1995; Brown and Woodfill, 1998).

**Figure 4.** Lithologic interpretation, gamma-ray, neutron density, sonic, and synthetic seismogram (30 Hz, zero phase Ricker wavelet) from the Arco-Marathon Paul Gibbs #1 well.

**Figure 5.** (A) Uninterpreted seismic reflection profile 83-201V. The vibroseis sourced profile is the northernmost seismic line, and crosses the Lewis thrust. The profile is time migrated and stretched to depth with no vertical exaggeration. (B) A structural interpretation of 83-201V. Strong reflections are in the upper half of the data, suggesting stratigraphical change. The RMBD is located near -8 km elevation and the sole point of the Lewis thrust is visible. Two other major faults are visible, the Hefty thrust and the MacDonald thrust. RMBD – RMBD, HT – Hefty thrust, MF – MacDonald thrust, Ylb – lower Belt, Yr – Ravalli group, Yh –middle Belt, Ym – Missoula group, DCu – Devonian and Cambrian undivided, Mu – Mississippian, PPr – Pennsylvanian and Permian, Pz – Paleozoics undivided.

**Figure 6.** (A) Uninterpreted seismic reflection profile 83-101. This profile was collected using the Poulter method and it crosses the eastern Purcell Anticlinorium, RMT, Lewis thrust, and the Kishenehn Basin.

The seismic profile is post-stack depth migrated without vertical exaggeration. (B) A structurally balanced interpretation of Profile 83-101. The lower fault is identified as the RMBD, with the small wedge of autochthonous Belt rocks beneath until basement. Note the sole point of the Lewis thrust into the décollement zone. The RMTF system has a slip of ~3 km. The Hefty thrust is visible throughout the profile with a slip of ~5.5 km. Coherent reflections on the western section of the profile have been interpreted as sills (marked with an S). RMBD – RMBD, RMTF – RMT fault system, HT – Hefty thrust, NF- Nyack fault, Yb – autochthonous Belt, Ylb – lower Belt, Yr – Ravalli group, Yh –middle Belt, Ym – Missoula group, DCu – Devonian and Cambrian undivided, Mu – Mississippian, PPr – Pennsylvanian and Permian, Pz – Paleozoics undivided, Mz – Mesozoics undivided, T – Tertiary fill.

**Figure 7.** (A) Uninterpreted seismic reflection profile 83-103. The Poulter method profile crosses the Lewis thrust. The seismic profile is depth migrated and plotted without vertical exaggeration. (B) A structural interpretation of 83-103. The RMBD is labeled and is located at -7 km elevation to the east. The Lewis thrust sole point is interpreted, with Paleozoic rocks beneath. The Hefty thrust is visible throughout the profile with a slip of ~ 5.5 km. No autochthonous Belt rocks are interpreted in the seismic profile. RMBD – RMBD, HT – Hefty thrust, Ylb – lower Belt, Yr – Ravalli group, Yh –middle Belt, Ym – Missoula group, Pz – Paleozoics undivided.

**Figure 8.** (A) Uninterpreted seismic reflection Poulter method profile 83-104 that crosses the Rocky Mountain Trench. The data is time migrated and post-stack migrated, shown without vertical exaggeration. (B) A structural interpretation 83-104. Note the RMBD with the autochthonous Belt beneath. Also note in the top west of the profile a clearly defined boundary between the Tertiary fill and the Belt rock approximately 1 km deep. The profile is too far west to see any indication of the Lewis thrust sole point. The fault on the top of the profile was a thrust fault but has since been reactivated to form a normal fault. Major reflections on the western edge have been interpreted as sills (marked as an

S). RMBD – RMBD, RMTF – RMT fault system, WF – Whitefish fault, Ylb – lower Belt, Yr – Ravalli group, Yh –middle Belt, Ym – Missoula group, T – Tertiary fill.

**Figure 9.** (A) Uninterpreted seismic reflection profile 83-105. The Poulter method profile crosses the eastern Purcell Anticlinorium, RMT, and the Lewis thrust. The profile is shown without vertical exaggeration and is pre-stack time migrated. (B) A structurally balanced interpretation of 83-105. Note the location and offset of the RMT fault system with ~3.5 km of dip slip, and the major sills in the western section (marked with an S). The sole points of the Lewis thrust and the Hefty thrust into the RMBD are also shown. The Whitefish fault which has been reactivated as a normal fault is shown. RMBD – RMBD, RMTF – RMT fault system, WF – Whitefish fault, HT – Hefty thrust, Ylb – lower Belt, Yr – Ravalli group, Yh –middle Belt, Ym – Missoula group, Pz – Paleozoics undivided, T – Tertiary fill.

**Figure 10.** Schematic model illustrating the tectonic development of the RMT. A)The Belt basin and overlying Paleozoic rocks following deposition prior to tectonism (Proterozoic-Middle Jurassic). B) Compressional translation of the Belt basin onto a footwall hinge and formation of a structural high draped over the basin margin (Late Jurassic-Paleocene). C)Structural high becomes gravitationally unstable and begins to collapse (Paleocene-Eocene). D) RMT fault reactivates the basin margin décollement ramp (modified from van der Velden and Cook, 1996).

**Figure 11.** A simplified block diagram of the extensional slips of the Flathead fault and RMT fault systems from 50°N to 48.5°N, showing the faults structurally linked in an en echelon fault system. As the RMTF system extension decreases, the Flathead fault system extension increases, and vice versa. RMTF – RMT fault system, FF – Flathead fault system, KB -Kishenehn basin (Constenius, 1982, 1988; van der Velden and Cook, 1996)

**Table 1. Seismic Data Acquisition Parameters.**

	<u>83-201V</u>	<u>83-101, 83-103, 83-104, 83-105</u>
Station Interval (m)	50.3	50.3
Source Interval (m)	100.6	100.6
Group Interval (m)	50.3	50.3
Common Midpoint Interval (m)	25.1	25.1
Number of Channels	96	96
Recording Configuration	Split-dip spread	Split-dip spread
Nominal Stacking Fold	24	24
Recording Bandpass Filter (Hz)	16-128	12-128
Source Type	4 or 5 Seismic Vibrators	1 to 80 lbs. Tovex (Poulter Method)
Sweep Frequencies (Hz)	56→14	N/A
Sweep Length (s)	20	N/A
Source Repetition Per Location	15	1
Field Record Length (s)	20	5
Correlated Record Length (s)	5	N/A
Sample Interval (ms)	2	2

**Table 2. Seismic Data Processing Sequence.****83-201V**

- 1) Self-truncating extended correlation
- 2) Convert to minimum phase
- 3) Trace edit
- 4) Refraction and elevation statics computation  
Replacement velocity: 5000 m/s  
Processing datum: 2400 m
- 5) Gain compensation
  - i. Exponential gain function
  - ii. RMS scale in overlapping static windows
- 6) Surface consistent deconvolution
- 7) Top mute application
- 8) CMP stacking velocity analysis 1
- 9) Residual statics estimation 1
- 10) CMP stacking velocity analysis 2
- 11) Residual statics estimation 2
- 12) CMP stacking velocity analysis 3
- 13) THOR
- 13) Ormsby band pass filter (8:12,55:60 Hz)
- 12) Final CMP stack
- 14) Ormsby band pass filter (8:12,55:60 Hz)
- 15) PSTM velocity and aperture angle analysis
- 16) PSTM application
- 17) DM velocity model building
- 18) Stretch to depth (using DM velocity model)
- 19) Principle component based dip coherency

**83-101, 83-103, 83-104, 83-105**

- 1) Trace edit
- 2) Refraction and elevation statics computation  
Replacement velocity: 5000 m/s  
Processing datum: **83-101:** 2400 m, **83-103:** 2300 m, **83-104:** 2400 m, **83-105:** 2400 m
- 3) Gain compensation
  - i. Exponential gain function
  - ii. RMS scale in overlapping static windows
- 4) Trace balance
- 5) Surface consistent deconvolution
- 6) Top and tail mute application
- 7) CMP stacking velocity analysis 1
- 8) Residual statics estimation 1
- 9) CMP stacking velocity analysis 2
- 10) Residual statics estimation 2
- 11) CMP stacking velocity analysis 3
- 12) THOR
- 13) Ormsby band pass filter (8:12,55:60 Hz)
- 14) Final CMP stack
- 15) PSTM velocity analysis and aperture angle analysis
- 16) PSTM application
- 17) DM velocity model building and aperture angle analysis
- 18) DM application (pre or post stack depth migration)
- 19) Principle component based dip coherency

**RMS:** root mean squared, **CMP:** common midpoint, **THOR:** Threshold median removal of strong noise [Butler, 2012] , **PSTM:** prestack time migration, **DM:** depth migration

## Illustrations

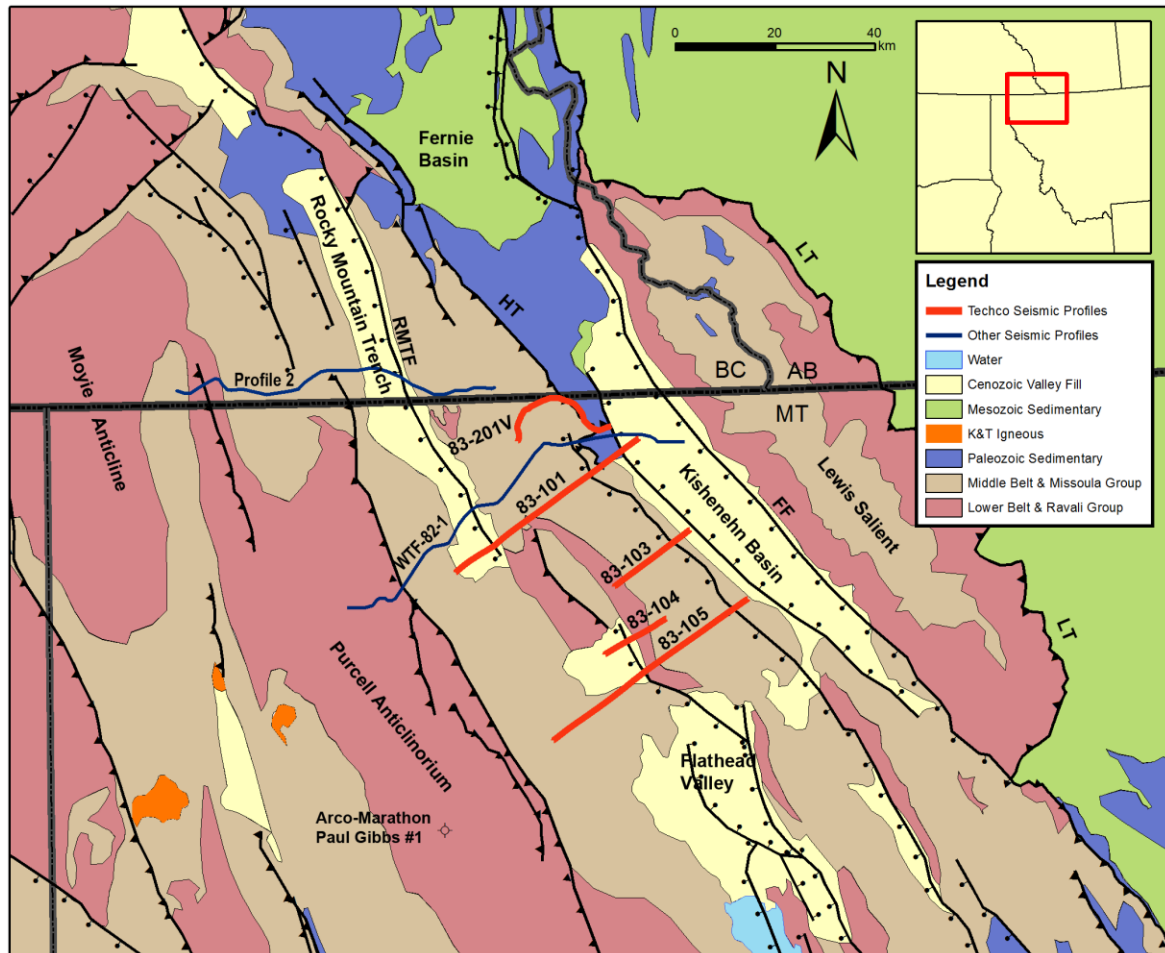


**Figure 1.** A simplified geologic map of northwestern Montana and nearby areas. The location of the reprocessed seismic lines and other seismic lines are shown. The Arco-Marathon well that proved the existence of sills is shown, as well as major geologic features and faults such as the Purcell Anticlinorium, Rocky Mountain Trench, Kishenehn Basin, and the Lewis Salient. RMTF – RMT fault, HT – Hefty thrust, FF – Flathead fault (Harrison et al., 1986; Harrison et al., 1992; Harrison et al., 1998; Mudge et al., 1982; van der Velden and Cook, 1994; Massey et al., 2005; Vuke et al., 2007).

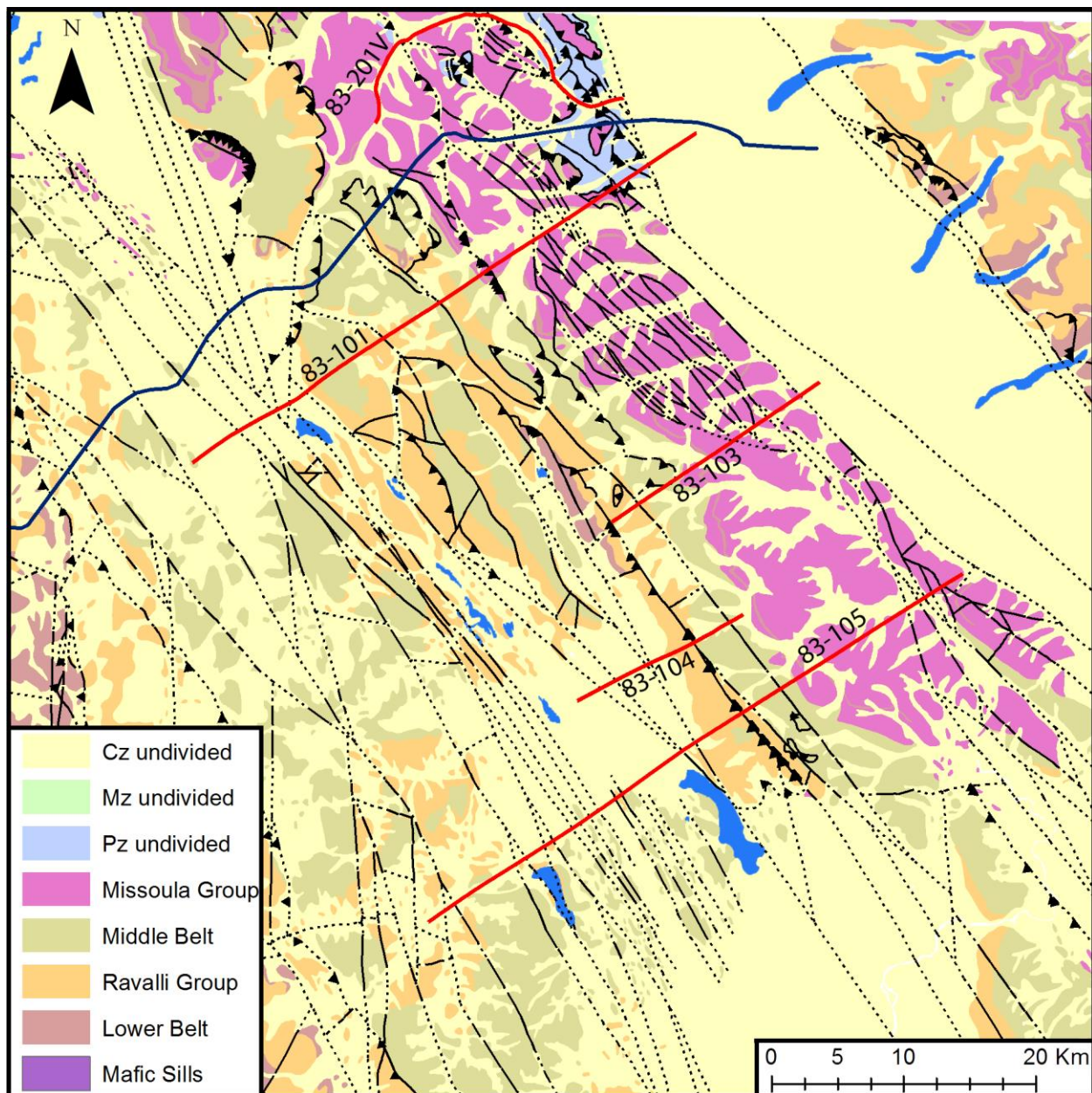


**Figure 2.** Detailed geologic map of the study area where the seismic data were collected. This map provided the surface data used in the interpretation of the profiles (modified from Harrison et al., 1992).

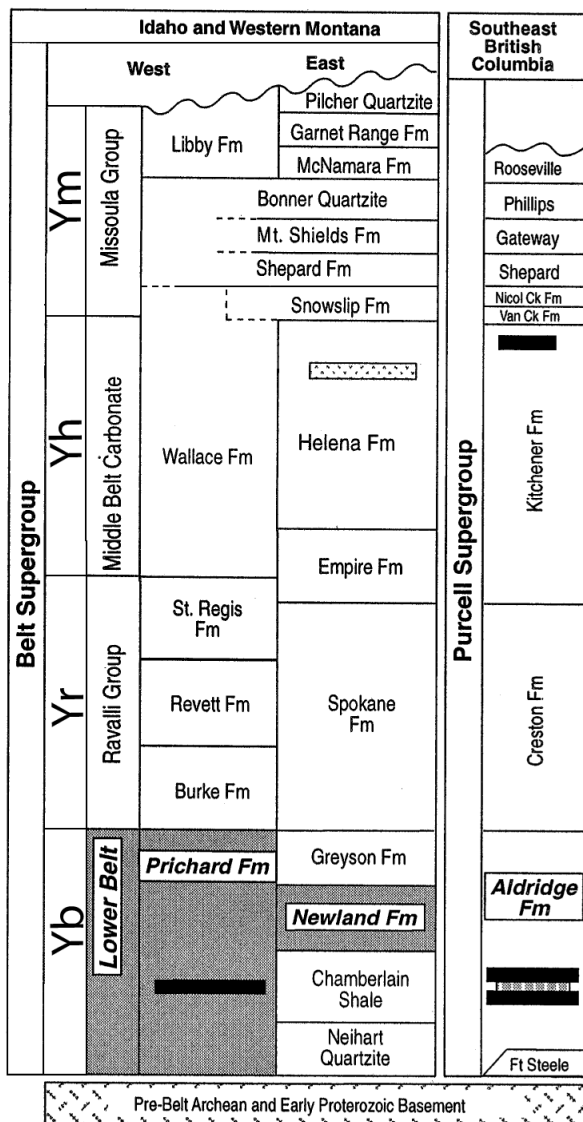


**Figure 3.** Regional stratigraphic column and geochronometric ages of Belt-Purcell Supergroup strata. The lower Belt is frequently intruded by sills approximately 1400 Ma (modified from Anderson and Davis, 1995; Brown and Woodfill, 1998; Luepke and Lyons, 2001).

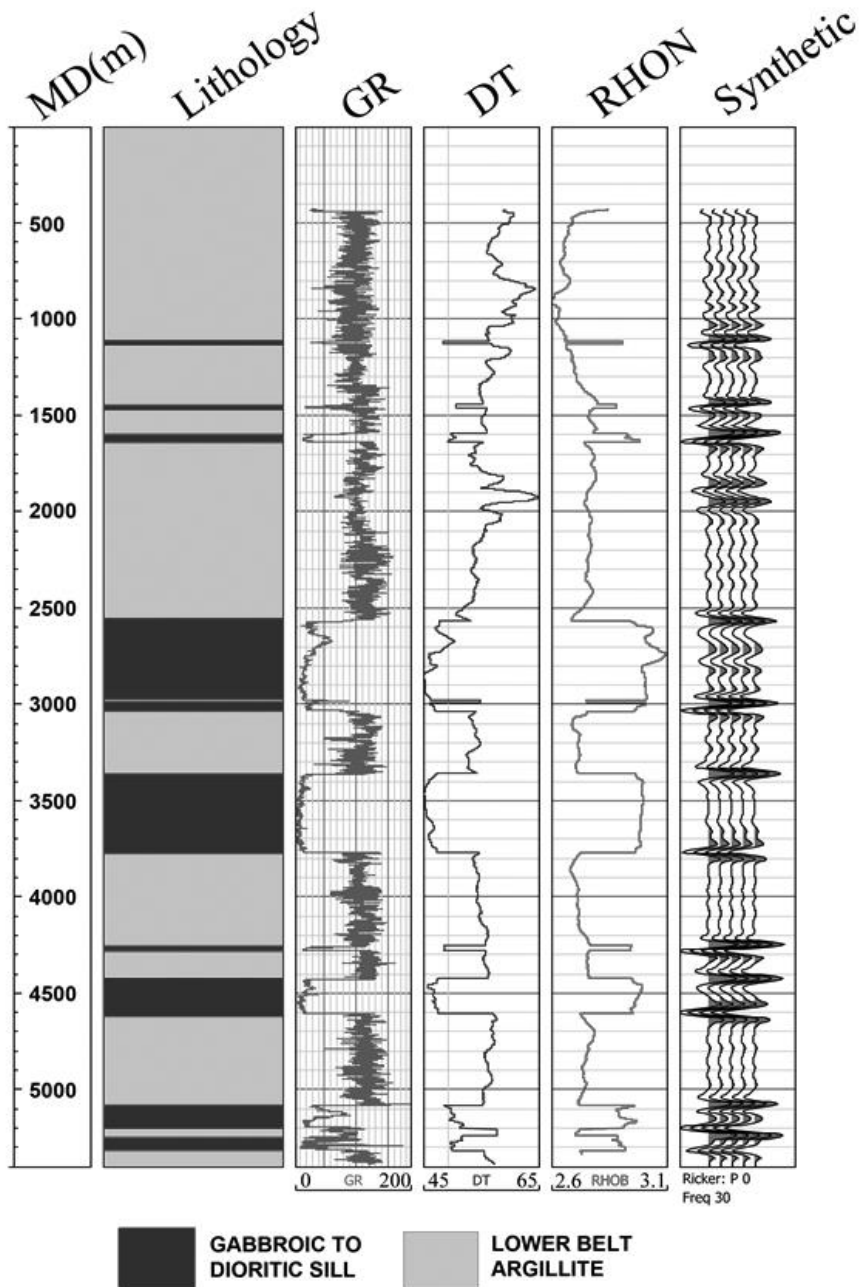


**Figure 4.** Lithologic interpretation, gamma-ray, neutron density, sonic, and synthetic seismogram (30 Hz, zero phase Ricker wavelet) from the Arco-Marathon Paul Gibbs #1 well.



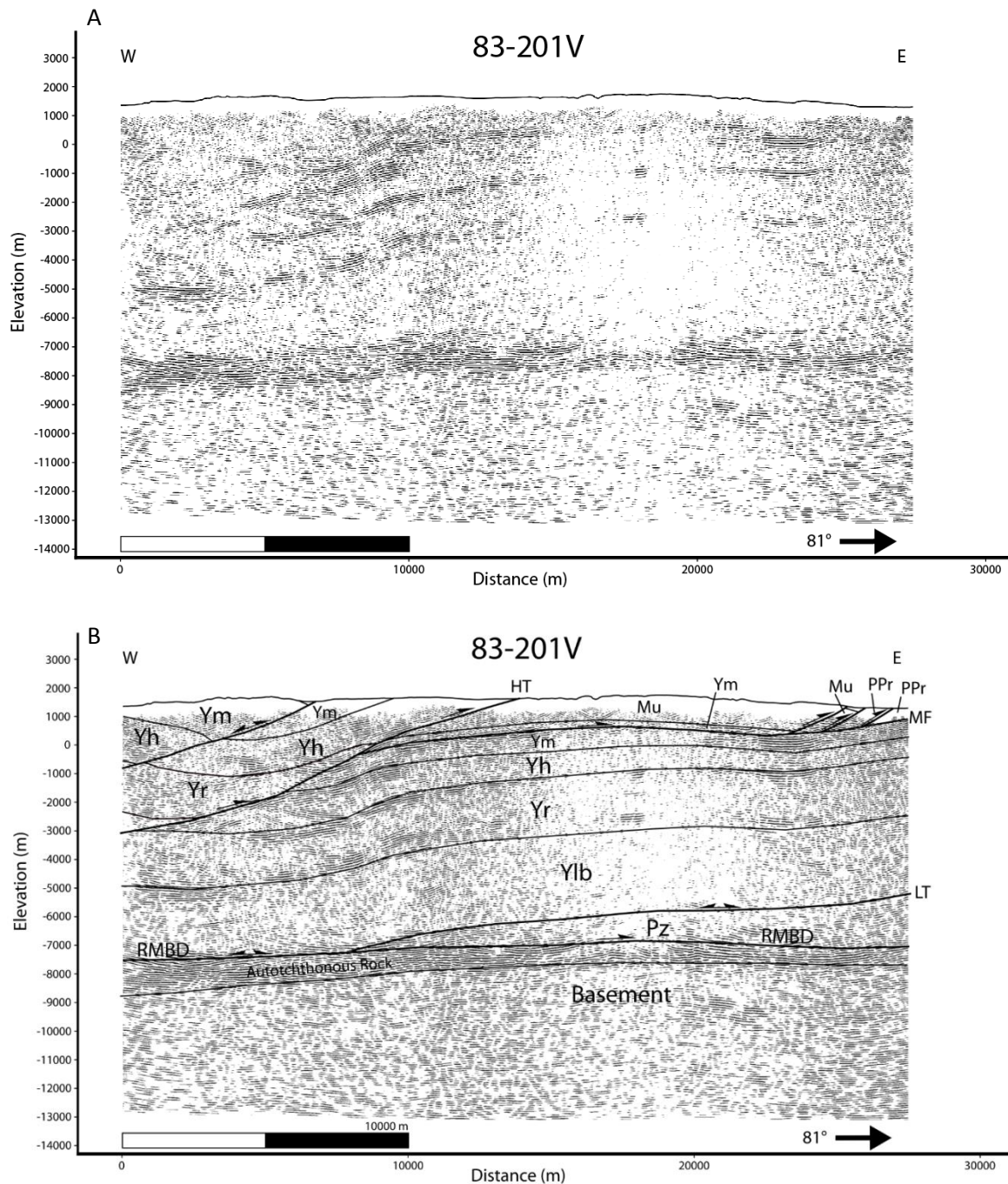


**Figure 5.** (A) Uninterpreted seismic reflection profile 83-201V. The vibroseis sourced profile is the northernmost seismic line, and crosses the Lewis thrust. The profile is time migrated and stretched to depth with no vertical exaggeration. (B) A structural interpretation of 83-201V. Strong reflections are in the upper half of the data, suggesting stratigraphical change. The RMBD is located near -8 km elevation and the sole point of the Lewis thrust is visible. Two other major faults are visible, the Hefty thrust and the MacDonald thrust. RMBD – RMBD, HT – Hefty thrust, MF – MacDonald thrust, Ylb – lower Belt, Yr – Ravalli group, Yh – middle Belt, Ym – Missoula group, DCu – Devonian and Cambrian undivided, Mu – Mississippian, PPr – Pennsylvanian and Permian, Pz – Paleozoics undivided.

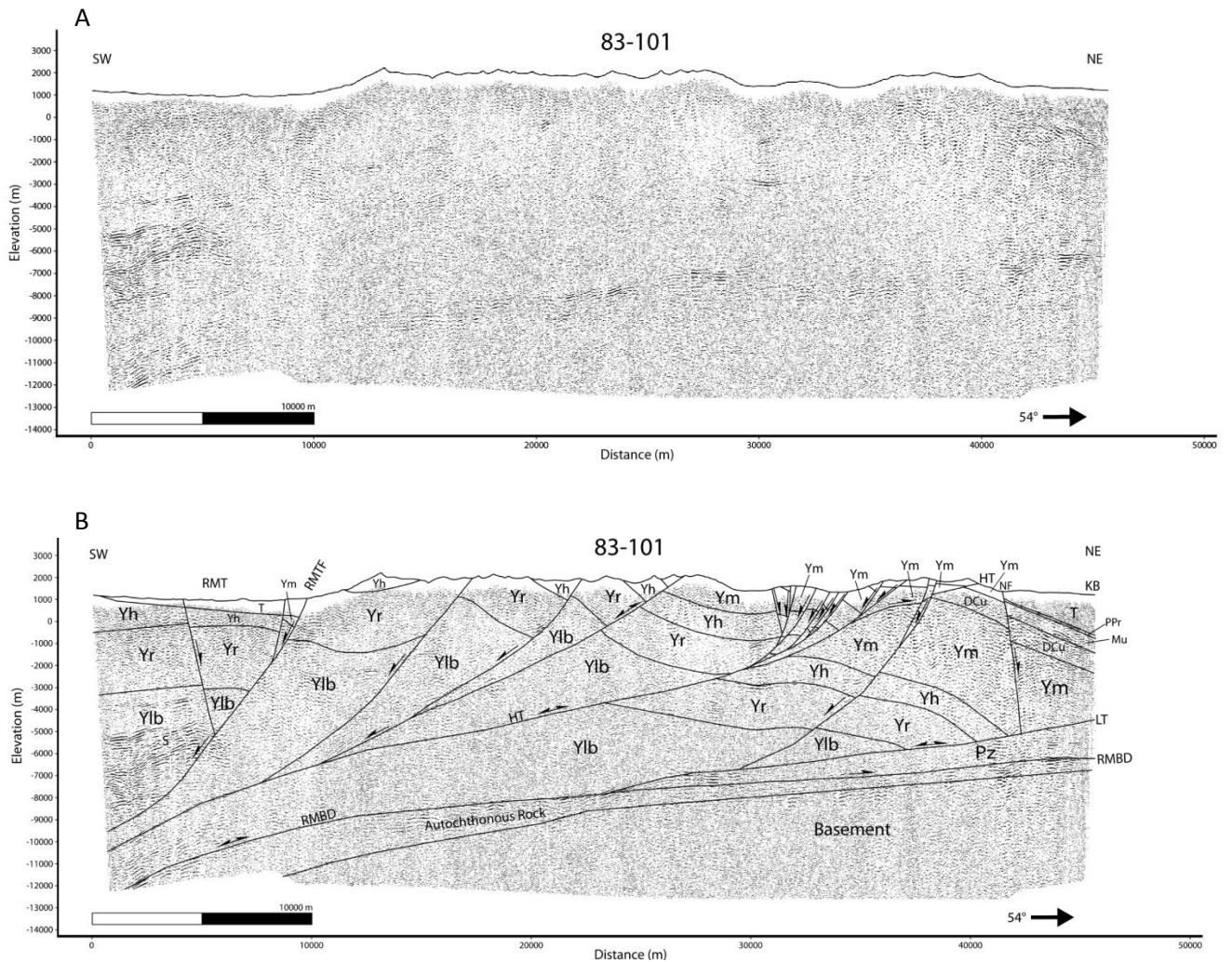


**Figure 6.** (A) Uninterpreted seismic reflection profile 83-101. This profile was collected using the Poulter method and it crosses the eastern Purcell Anticlinorium, RMT, Lewis thrust, and the Kishenehn Basin. The seismic profile is post-stack depth migrated without vertical exaggeration. (B) A structurally balanced interpretation of Profile 83-101. The lower fault is identified as the RMBD, with the small wedge of autochthonous Belt rocks beneath until basement. Note the sole point of the Lewis thrust into the décollement zone. The RMTF system has a slip of ~3 km. The Hefty thrust is visible throughout the profile with a slip of ~5.5 km. Coherent reflections on the western section of the profile have been interpreted as sills (marked with an S). RMBD – RMBD, RMTF – RMT fault system, HT – Hefty thrust, NF – Nyack fault, Yb – autochthonous Belt, Ylb – lower Belt, Yr – Ravalli group, Yh – middle Belt, Ym – Missoula group, DCu – Devonian and Cambrian undivided, Mu – Mississippian, PPr – Pennsylvanian and Permian, Pz – Paleozoics undivided, Mz – Mesozoics undivided, T – Tertiary fill.

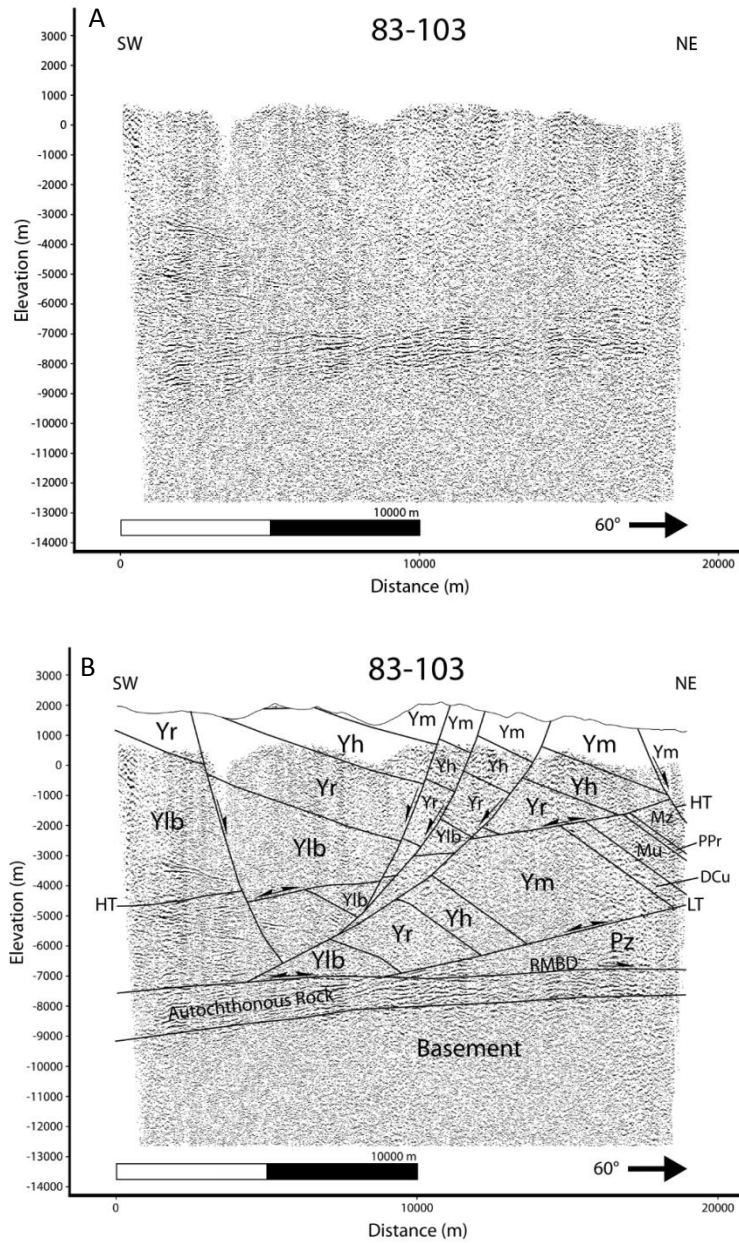


**Figure 7.** (A) Uninterpreted seismic reflection profile 83-103. The Poulter method profile crosses the Lewis thrust. The seismic profile is depth migrated and plotted without vertical exaggeration. (B) A structural interpretation of 83-103. The RMBD is labeled and is located at -7 km elevation to the east. The Lewis thrust sole point is interpreted, with Paleozoic rocks beneath. The Hefty thrust is visible throughout the profile with a slip of ~5.5 km. No autochthonous Belt rocks are interpreted in the seismic profile. RMBD – RMBD, HT – Hefty thrust, Ylb – lower Belt, Yr – Ravalli group, Yh –middle Belt, Ym – Missoula group, Pz – Paleozoics undivided.

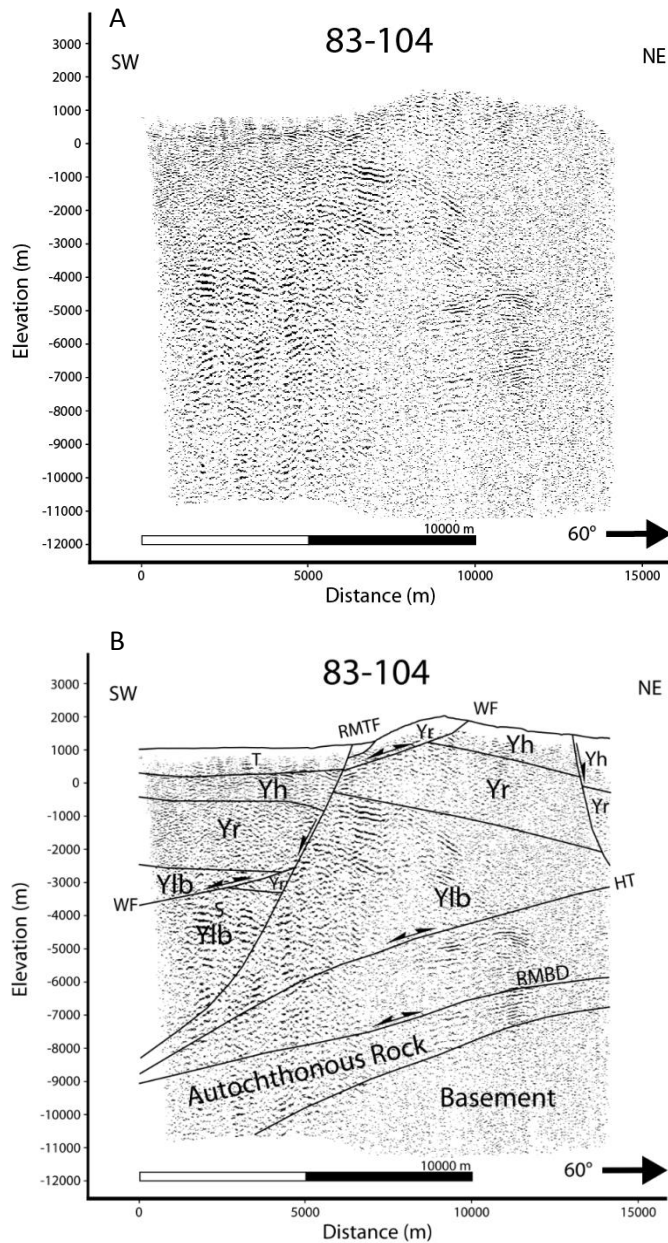


**Figure 8.** (A) Uninterpreted seismic reflection Poulter method profile 83-104 that crosses the Rocky Mountain Trench. The data is time migrated and post-stack migrated, shown without vertical exaggeration. (B) A structural interpretation 83-104. Note the RMDB with the autochthonous Belt beneath. Also note in the top west of the profile a clearly defined boundary between the Tertiary fill and the Belt rock approximately 1 km deep. The profile is too far west to see any indication of the Lewis thrust sole point. The fault on the top of the profile was a thrust fault but has since been reactivated to form a normal fault. Major reflections on the western edge have been interpreted as sills (marked as an S). RMDB – RMDB, RMTE – RMT fault system, WF – Whitefish fault, Ylb – lower Belt, Yr – Ravalli group, Yh –middle Belt, Ym – Missoula group, T – Tertiary fill.

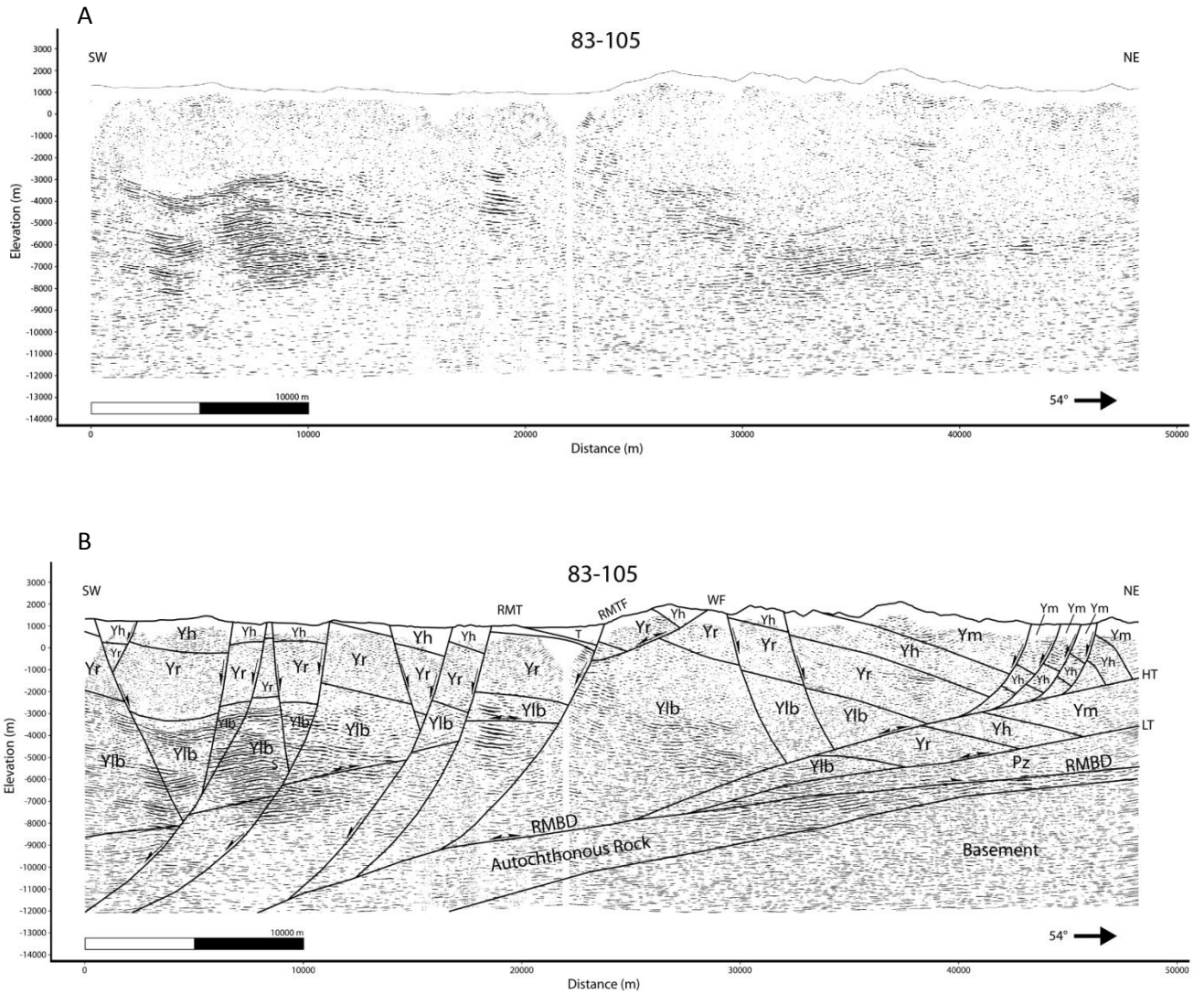


**Figure 9.** (A) Uninterpreted seismic reflection profile 83-105. The Poulter method profile crosses the eastern Purcell Anticlinorium, RMT, and the Lewis thrust. The profile is shown without vertical exaggeration and is pre-stack time migrated. (B) A structurally balanced interpretation of 83-105. Note the location and offset of the RMT fault system with ~3.5 km of dip slip, and the major sills in the western section (marked with an S). The sole points of the Lewis thrust and the Hefty thrust into the RMBD are also shown. The Whitefish fault which has been reactivated as a normal fault is shown. RMBD – RMBD, RMTF – RMT fault system, WF – Whitefish fault, HT – Hefty thrust, Ylb – lower Belt, Yr – Ravalli group, Yh – middle Belt, Ym – Missoula group, Pz – Paleozoics undivided, T – Tertiary fill.

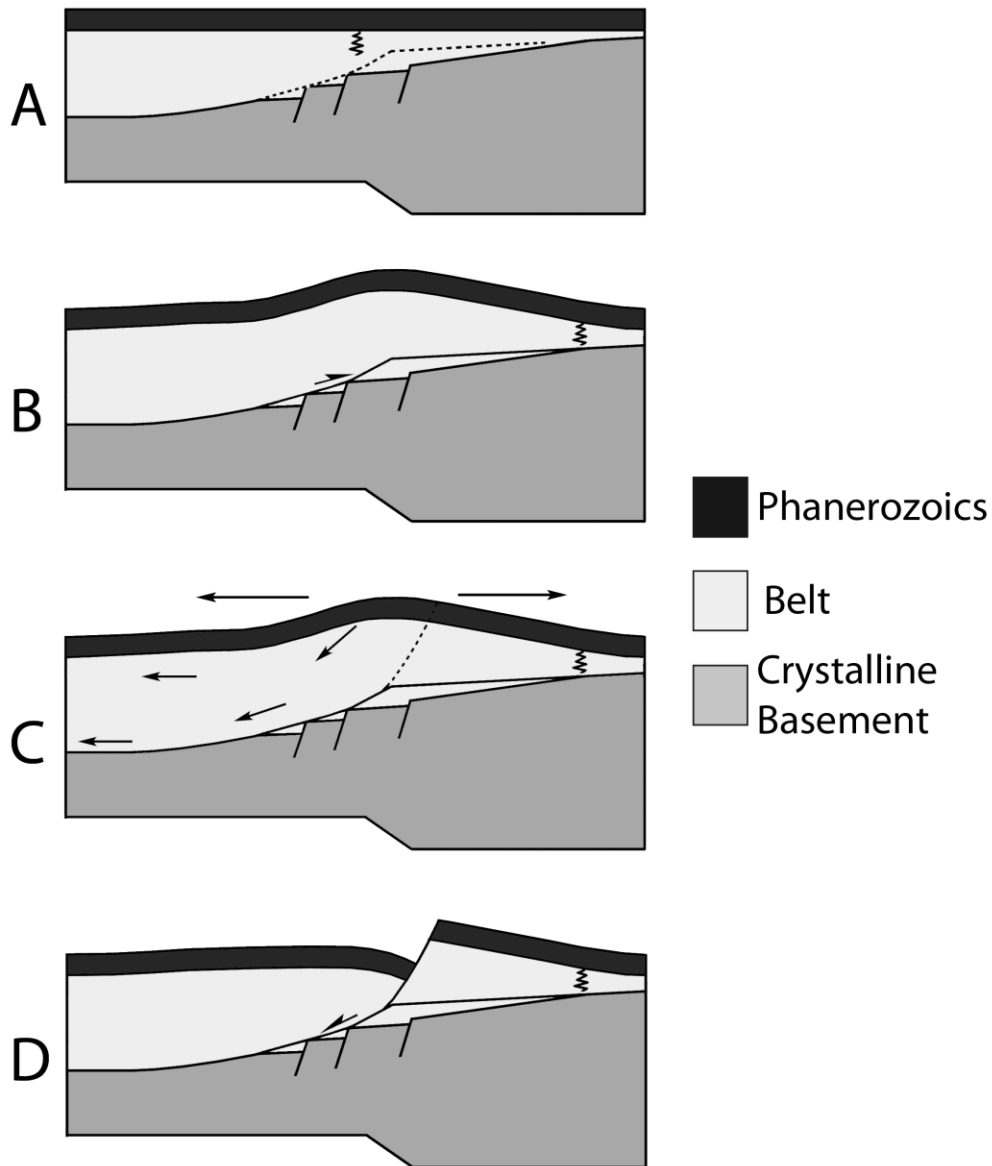


**Figure 10.** Schematic model illustrating the tectonic development of the RMT. A) The Belt basin and overlying Paleozoic rocks following deposition prior to tectonism (Proterozoic-Middle Jurassic). B) Compressional translation of the Belt basin onto a footwall hinge and formation of a structural high draped over the basin margin (Late Jurassic-Paleocene). C) Structural high becomes gravitationally unstable and begins to collapse (Paleocene-Eocene). D) RMT fault reactivates the basin margin décollement ramp (modified from van der Velden and Cook, 1996).



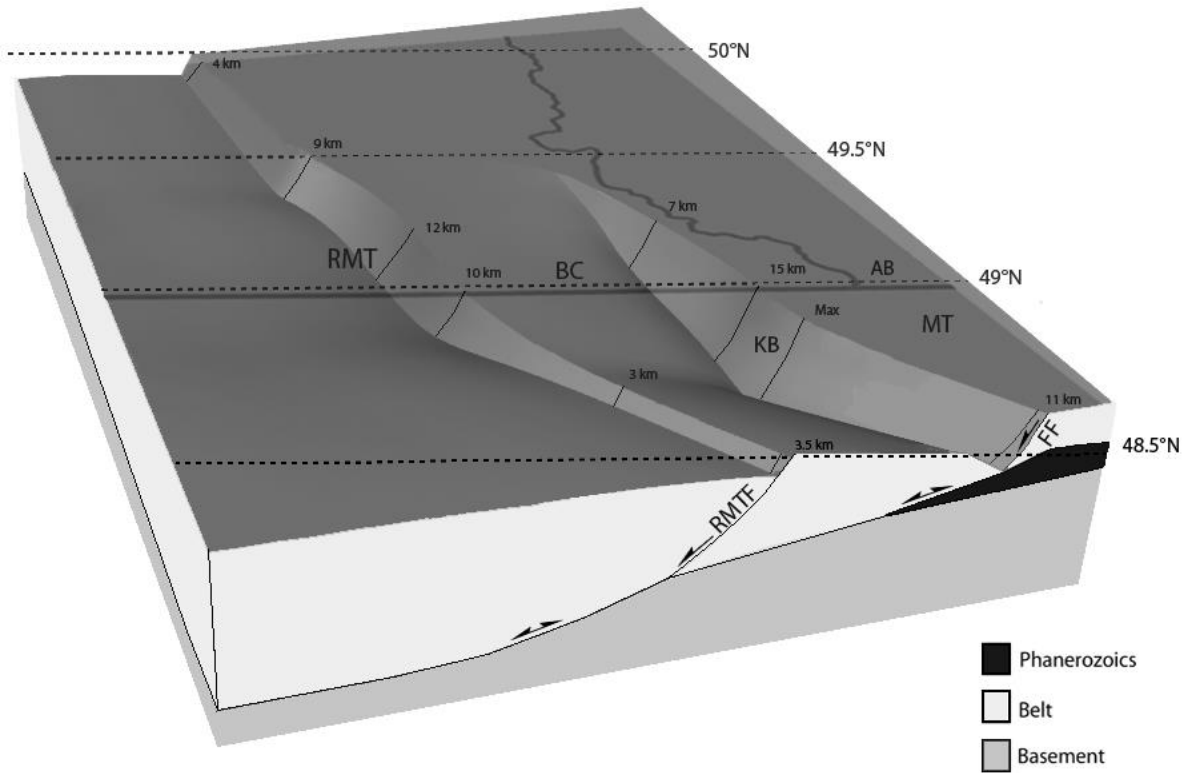


**Figure 11.** A simplified block diagram of the extensional slips of the Flathead fault and RMT fault systems from 50°N to 48.5°N, showing the faults structurally linked in an en echelon fault system. As the RMTF system extension decreases, the Flathead fault system extension increases, and vice versa. RMTF – RMT fault system, FF – Flathead fault system, KB -Kishenehn basin (Constenius, 1982, 1988; van der Velden and Cook, 1996)